Review

Chirality at the Nanoparticle Surface: Functionalization and Applications

Muhammad Shajih Zafar [1] and Andrea Ragusa [2,3,*]

1   Department of Engineering for Innovation, University of Salento, via Monteroni, 73100 Lecce, Italy; muhammad.zafar@iit.it
2   CNR Nanotec, Institute of Nanotechnology, via Monteroni, 73100 Lecce, Italy
3   Department of Biological and Environmental Sciences and Technologies, University of Salento, via Monteroni, 73100 Lecce, Italy
*   Correspondence: andrea.ragusa@unisalento.it; Tel.: +39-0832-319208

check for updates

Abstract: Chiral molecules, such as amino acids and carbohydrates, are the building blocks of nature. As a consequence, most natural supramolecular structures, such as enzymes and receptors, are able to distinguish among different orientations in space of functional groups, and enantiomers of chiral drugs usually have different pharmacokinetic properties and physiological effects. In this regard, the ability to recognize a single enantiomer from a racemic mixture is of paramount importance. Alternatively, the capacity to synthetize preferentially one enantiomer over another through a catalytic process can eliminate (or at least simplify) the subsequent isolation of only one enantiomer. The advent of nanotechnology has led to noteworthy improvements in many fields, from material science to nanomedicine. Similarly, nanoparticles functionalized with chiral molecules have been exploited in several fields. In this review, we report the recent advances of the use of chiral nanoparticles grouped in four major areas, i.e., enantioselective recognition, asymmetric catalysis, biosensing, and biomedicine.

Keywords: chirality; enantiomers; chiral nanoparticle; supramolecular chemistry; asymmetric catalysis; enantioselective recognition; biomedicine; biosensor

1. Introduction

Chirality plays a major role in nature. It is almost ubiquitous because of the presence chiral building blocks, such as carbohydrates and amino acids, used for the creation of advanced covalent and supramolecular structures, i.e., proteins, enzymes, and glycoconjugates (such as glycoproteins and glycolipids) [1]. As such, most bioactive species exhibit chiral features and many key biological mechanisms possess specific interactions with chiral molecules [2–4]. Up until now, the source of homochirality in the monomeric units of biopolymers in nature is one of the main scientific queries that still remains unexplained. The motive as to why only L-amino acids and D-monosaccharides are present in alive organisms is still unknown. The choice of a single enantiomer in biomolecules, e.g., by impulsive self-assembling into planned shapes, is a procedure that is not yet clear [5].

Chiral recognition also plays a key part in the field of chemical, biological, and pharmaceutical sciences because of the precise orientation of functional groups in chiral molecules [6–9]. Many active pharmaceutical ingredients (APIs) are chiral and the two enantiomers often present different pharmacokinetic, therapeutic, and toxicological profiles. Since the application of 1990s guidelines about stereochemistry in drug discovery and development, most drug companies and research institutes have focused their attention on single enantiomers. Furthermore, many active enantiomers of drugs

that are already commercialized in racemic mixture have been patented as single APIs as soon as the old patent expired, a phenomenon known as chiral switching [10].

Advances in nanotechnology have led to an ever-increasing fabrication and consumption of engineered nanoparticles (NPs) and the enormous steps made forward in material science and medical applications have been extensively acknowledged [11–14]. Chiral molecules adsorbed on an appropriate surface show a significant role in stereoselective heterogeneous catalysis [15] and material science [16].

Chiral NPs have been known since 2007, when Jadzinsky et al. determined the structure of a 102-atom gold nanoparticle (Au NP) covered with 44 *p*-mercaptobenzoic acid molecules and noted a symmetric *fcc* core surrounded by an asymmetric shell of Au atoms bound to the thiol of the ligands, thus yielding inherently chiral NPs with the two enantiomers alternating in the crystal lattice [17]. More recent studies have evidenced that achiral metallic nanoparticles show chiral properties that are determined by amino acids and peptides bound to their surface. As a consequence, such NPs can produce strong chiral optical signals even at visible wavelengths and they could be exploited for a variety of applications, from enantioselective recognition to asymmetric catalysis and sensing, as well as biomedicine.

In this article, we review the recent applications of chiral NPs. We concentrated our attention on the molecules employed for functionalizing the surface of the NPs and the way in which they allow for the obtaining of specific interactions with the host in solution. In general, metallic NPs have been used, such as gold and silver NPs, or magnetic NPs, for exploiting their ability to be attracted by an external magnetic field and separate enantiomeric species, or quantum dots (i.e., CdSe/CdS core-shell NPs) for taking advantage of their photoluminescent capacity. On the other hand, carbohydrates and amino acids are the main, but not the only, ligands used for obtaining the enantioselective interaction.

2. Applications of Chiral Nanoparticles

2.1. Enantioselective Recognition

Enantioselective recognition of racemates through supramolecular assemblies has been widely investigated in the last decades in order, for example, to mimic nature or to simplify the purification process [18–22]. Chiral interactions are fundamental in most drugs and often only one enantiomer has pharmacological activity, the other one being not active or even toxic. That is why purification of racemic mixtures is of paramount importance. More recently, nanotechnology also explored this field, trying to help to reach these goals by combining the intrinsic physico-chemical properties of NPs with those of organic receptors and ligands. The main findings of these studies are summarized in Table 1.

Table 1. Main applications of chiral NPs through enantioselective recognition and their principal characteristics.

NPs	Surface Functionalization	Application	Molecule Recognized	Reference
Au	cysteine	enantioselective recognition	propylene oxide	[23]
Tetrahexahedral Au	cysteine	enantioselective recognition	propranolol	[24]
Fe_3O_4/SiO_2	carboxymethyl-β-cyclodextrin	chromatographic separation	L-Trp, L-Phe, L-Tyr	[25,26]
Au/SiO_2	β-cyclodextrin	chromatographic separation	pesticides and drugs	[27]
Fe_3O_4	BSA	magnetic separation	ibuprofen, ofloxacin	[28]
Fe_3O_4/SiO_2	teicoplanin	magnetic separation	(+)-Trp, (+)-Phe	[29]

Table 1. *Cont.*

NPs	Surface Functionalization	Application	Molecule Recognized	Reference
Au/SiO$_2$	β-cyclodextrin	chromatographic separation	meptazinol	[30]
Au Janus NPs	hexanethiolates (hydrophobic side) and 3-mercapto-1,2-propandiol (hydrophilic side)	enantioselective recognition	D-cysteine	[31]
Ag nanohelices	benzenacyclotricosaphane-(1,2-dithiolan-3-yl)pentanoate derivative [1]	enantioselective recognition	chiral binaphthyl chromophore	[32]
Ag	cysteine	self-assembly	-	[33]
Ag and Au	C16-threonine dipeptide	self-assembly	-	[34]

[1] Complete chemical name: 3,6,9,12,14,17,20,23-octaoxa-1,2(1,2)-dinaphthalena-13(1,3)-benzenacyclotricosaphane-13^5-ylmethyl 5-(1,2-dithiolan-3-yl)pentanoate.

For example, Shukla and colleagues functionalized Au NPs with either D- or L-cysteine, which were used as enantioselective adsorbents of racemic propylene oxide that caused an increase in the optical rotation [23]. The authors managed to quantitatively determine the enantiospecific ratios of the adsorbed species by measuring the enantiospecific equilibrium constants, $K_L^S/K_D^S = K_D^R/K_L^R$ (where the subscript represents the chirality of the ligand–NP complex and the superscript that of the adsorbed species), without the need to know the surface area of the NPs (Figure 1). They later prepared tetrahexahedral Au NPs, again capped with D- or L-cysteine, for the enantioselective separation of the chiral pharmaceutical propranolol, an antihypertensive drug [24].
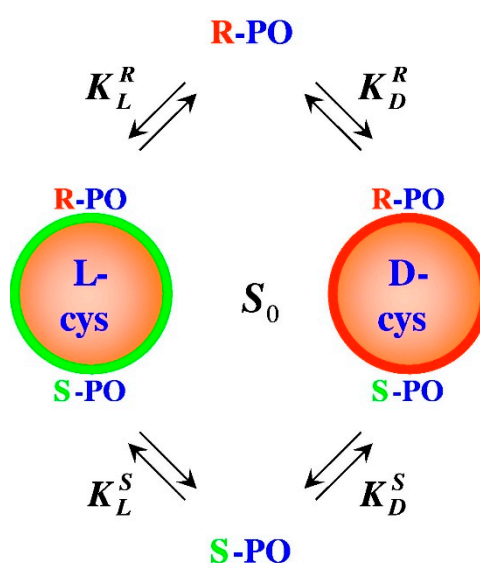
Figure 1. Recognition system developed by Shukla and colleagues. Reprinted with permission from [23], Copyright Elsevier, 2014.

Over the past decade, production of superparamagnetic nanoparticles has been extensively investigated, not only for its essential scientific interest but also for many technological applications such as medical imaging [35,36], magnetic field supported transport [37–39], and separations [40,41]. Similarly, they were also employed for separating racemic mixtures. Benefits of magnetic separation over more traditional methods are related to its rapidity, easiness, and cost-effectiveness.

Gosh et al. synthetized silica-encapsulated magnetic nanoparticles (MNPs) functionalized on their surface with carboxymethyl-β-cyclodextrin (CD) for the enantioselective recognition of aromatic amino acids [25]. The Fe$_3$O$_4$/SiO$_2$/CD MNPs, with the chiral properties of the β-CD and the biocompatibility

and superparamagnetism of iron oxide, could selectively adsorb amino acid enantiomers (L-Trp > L-Phe > L-Tyr and with much stronger binding force as compared to the corresponding D enantiomers) through host–guest interactions. The authors also showed that the CD MNPs selectively adsorbed the L enantiomers from racemic Trp, Phe, and Tyr with enantiomeric excess (e.e.) of 94%, 73%, and 58%, respectively, as determined by chromatographic method [26]. Enantioselectivity was shown to be mainly due to hydrogen bonding between the amine in α to the chiral center of the amino acid and the secondary hydroxyl groups of CD.

Silica spheres were also functionalized on their surface with β-cyclodextrin-capped Au NPs (about 60 nm in diameter) by Li and colleagues, and they were used as chiral selectors for the enantioseparation of several chiral pesticides and drugs by HPLC [27]. The presence of Au NPs improved the overall efficiency of the system compared to traditional β-CD-modified silica column and could be easily applied to the separation of additional racemic mixtures.

Fu and colleagues also exploited MNPs for separating chiral drugs, a fundamental step in the pharmaceutical industry [28]. Bovine serum albumin (BSA) anchored to the NPs surface was able to recognize ibuprofen and ofloxacin with an e.e. of 13% and 14% for single-stage adsorption, respectively, and e.e. values of 54% and 39% for multi-stage operation, respectively. A hybrid procedure combining the magnetic enantiomeric enrichment followed by crystallization allowed for the obtaining of an even higher optical purity (up to 99% e.e. for ibuprofen).

Mesoporous silica MNPs functionalized on the outer surface with teicoplanin, an antibiotic glycopeptide, showed excellent chiral selectivity and separation ability from racemic solutions of aromatic amino acids using an exterior magnetic field [29]. Much stronger interactions were stabilized with the (+)-enantiomers, compared to the (−)-enantiomers, of tryptophan and phenylalanine, and the system was also shown to be highly stable and reusable (Figure 2).

Fe$_3$O$_4$ MNPs

Teicoplanin

• (+)-enantiomers
■ (-)-enantiomers
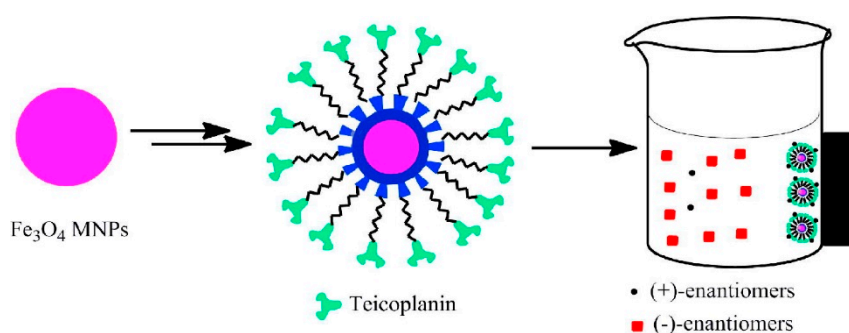
Figure 2. Magnetic separation of (+)-Trp and (+)-Phe by means of teicoplanin-functionalized MNPs. Reprinted with permission from [29], Copyright Elsevier, 2013.

Layer-by-layer self-assembly of cyclodextrin-coated Au NPs onto silica spheres was also exploited as stationary phase for the chiral recognition and separation of meptazinol from its three enantiomers by capillary electrochromatography [30]. The methodology was shown to possess good linearity (≥0.999), recovery (92.0–94.5%), and repeatability, and it was efficiently employed for the enantioseparation of meptazinol in spiked urine samples.

Utilizing a different approach, Lu and colleagues prepared gold Janus nanoparticles covered by (hydrophobic) hexanethiolates and (hydrophilic) 3-mercapto-1,2-propandiol that displayed positive circular dichroism (CD) absorption in the visible range following the selective encapsulation of enantiomers into the emulsion cavities of the NP [31]. In particular, D-cysteine resulted as the favored enantiomer trapped into the emulsions, where the ligand exchange reaction occurred at the hydrophilic face of the Janus NPs. By controlling concentration and reaction time, chiral Janus nanoparticles could be also prepared by ligand exchange reactions utilizing a racemic mixture of ligands.

Enantioselective recognition was also exploited for amplifying the optical activity of chiral molecules by using chiral ligands containing the binaphthyl chromophore anchored on the surface of

Ag NPs with a sub-5 nm helical pitch (*P*) [32]. The amplification was attributed to the enantiospecific adsorption of the ligand, which caused a variation of the dihedral angle of the binaphthyl chromophore, thus transferring the chiral signal of the Ag NPs to the binaphthyl chromophore through the Ag–S bicontacts. This enantioselective amplification did not happen on the Ag NPs without chiral footprint or on the chiral Ag NPs with a nominal *P* > 5 nm because of the dimensional mismatch of the footprints and the Ag–S bicontacts.

Chiral recognition can also lead to particular self-assembled tridimensional structures. For example, Rezanka and colleagues prepared silver nanoparticles (≈45 nm) functionalized with cysteine and *N*-, *C*-, and *S*-protected cysteine derivatives and observed the formation of an uncommon chiral architecture regardless of the enantiomer employed [33]. The authors noted that the assembly produced chiral electronic CD spectra, caused by optical molecular dipoles between the amino acids with a primary amine and the metallic core, and that the formation of the assembly depended on the concentration of the NPs and on the pH of the solution. These findings are in agreement with a model developed by Govorov et al. for calculating the electronic CD spectra of chiral molecule–nanoparticle complexes and who discovered that the intensity and shape of the of the absorption bands depends on the angle between the molecule and the surface of the NPs [42].

Self-assembling peptides have also been exploited for synthesizing Au and Ag NPs. In particular, the stereochemistry of L- and D-threonine caused β-sheets twisting in two artificial β-sheet dipeptides with long alkyl chains covering helical nanofibers that amplified supramolecular helicity (Figure 3) [34]. Furthermore, the hydrogen bonds among the amide groups and the hydrophobic interactions among the alkyl chains were shown to have a significant role in the progression of the self-assembled structure.
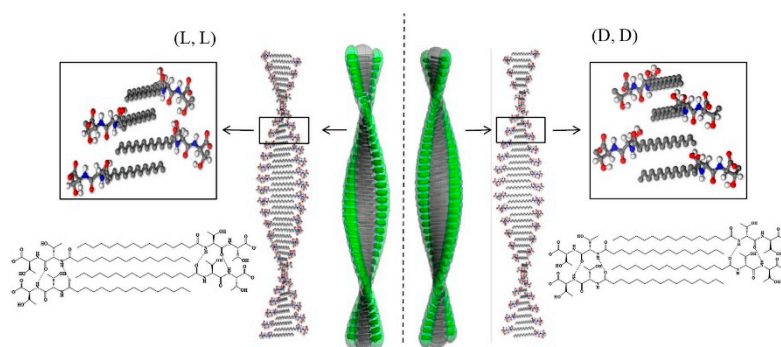
Figure 3. Mechanism of formation of helical structures for (L, L) and (D, D) threonine. Reprinted with permission from [34], Copyright Elsevier, 2016.

2.2. Asymmetric Catalysis

Catalysis is the process by which a chemical compound, the catalyst, is able to facilitate the conversion of the substrate into the product by lowering the energy of activation of the reaction. Eventually, the reaction can also be stereoselective if the catalyst is chiral.

Chemical ways to obtain enantio-enriched, and eventually enantiopure, products have attracted great attention over the past decades, inspiring extraordinary development in enantioselective catalysis, for example for the synthesis of enantiomerically pure pharmaceuticals or chemical products. This research led in 2001 to the award of the Nobel Prize for Chemistry to Noyori and Knowles, and Sharpless, for their work on asymmetric hydrogenation and oxidation reactions, respectively [43,44]. Numerous approaches have been investigated for obtaining heterogeneous enantioselective catalysts that could associate high catalytic activity to appropriate stereochemical mechanism of reaction, the most encouraging comprising alteration of the catalytic metal surface by a chiral compound with strong adsorbing capacity [45–47]. The high interest in heterogeneous enantioselective catalysis is also revealed by the ever-increasing number of research articles and by the amount of reviews on this topic [48–51]. More recently, nanotechnology has been also exploited for catalyzing chiral reactions as this modern approach can also help to override major hurdles of traditional catalyst,

for example purification [52]. The main finding about application of chiral NPs to asymmetric catalysis are summarized in Table 2.

Table 2. Main applications of chiral NPs for the asymmetric catalysis and their principal characteristics.

NPs	Surface Functionalization	Catalyzed Reaction	Reference
Ni	(*R*,*R*)-tartaric acid	carbonyl hydrogenation of β-ketoesters and β-diketoesters	[53]
Pt	CIL_{PEG-CD}	hydrogenation of activated ketones	[54]
$ZnCl_2/SiO_2$	*N*-myristoyl-L-alanine	hydroamination	[55]
Fe_3O_4	oxovanadium (+)-pseudoephedrine	oxidation of sulfides	[56]
Fe_3O_4	oxovanadium (+)-pseudoephedrine	carbonyl cyanosilylation	[57]
N-oleoyl-D/L-proline	-	aldol reaction	[58]
Fe_3O_4/SiO_2	cyclohexyl-1,2-diamine	aldol reaction	[59]
SiO_2	(*P*)-1,12-dimethyl-8-methoxycarbonylbenzo[*c*]phenantrene	Rh-catalyzed disulfide exchange	[60]
Au	triazacyclononane-Zn^{II}	RNA hydrolysis	[61]

One of the most extensively investigated reactions is the carbonyl hydrogenation of β-ketoesters and β-diketoesters over Ni-based catalysts in the presence of a chiral converter. Watson and co-workers adsorbed (*R*,*R*)-tartaric acid onto the surface of Ni NPs and exploited photoabsorption spectra to investigate in situ the chiral modification occurring during the catalysis reaction [53]. By means of scanning transmission X-ray microscopy combined with near-edge X-ray absorption fine structure spectroscopy (STXM/NEXAFS) they proposed that the tartaric acid placed onto the surfaces of the NPs from aqueous solutions experiences a ketoenol tautomerization. In addition, no "particle size effect" of the adsorption type of the tartaric acid was observed among NPs with a diameter between 90 and 300 nm.

Thermoregulated phase-separable Pt nanoparticle catalyst, functionalized with a cinchonidine derivative, also demonstrated excellent e.e. (>99%) in the enantioselective hydrogenation of activated ketones for synthesizing chiral α-hydroxy acetals and chiral 1,2-diols [54]. The chiral catalyst could be easily removed by phase separation and straightly recycled in the following process without losing its catalytic activity or enantioselectivity, even in a gram-scale reaction.

Hydroamination is another important synthetic method widely used for the preparation of chiral amines, very important functional groups in many APIs. Ng and colleagues attached $ZnCl_2$ on chiral mesoporous silica (Z-n-CMS, *n* = 1, 3, 5 mmol) obtaining strong Lewis acid catalysts on solid support for the hydroamination of cyclohexene [55]. The homogeneously dispersed $ZnCl_2$ nanoparticles (≈10 nm) presented catalytic synergistic outcome (>61% conversion) in the hydroamination of cyclohexene under mild conditions (60 °C) and the catalyst showed superior activity compared to other homogeneous and heterogeneous braced mesoporous catalysts seemingly because of the helical mesostructure that enhanced dispersion of the substrates and the availability of the Lewis acid sites.

Rostami et al. investigated the use of chiral oxovanadium (+)–pseudoephedrine complex sustained on Fe_3O_4 magnetic nanoparticles (VO(pseudoephedrine)@MNPs) as an innovative nanocatalyst for the chemoselective oxidation of sulfides to sulfoxides (Figure 4) [56]. By using hydrogen peroxide as a green oxidant, the reaction proceeded with high yields and enantiomeric excesses ranging between 20 and 27% at room temperature under solvent-free conditions. The catalyst was also recycled up to 20 times with minimal loss of action and enantioselectivity.
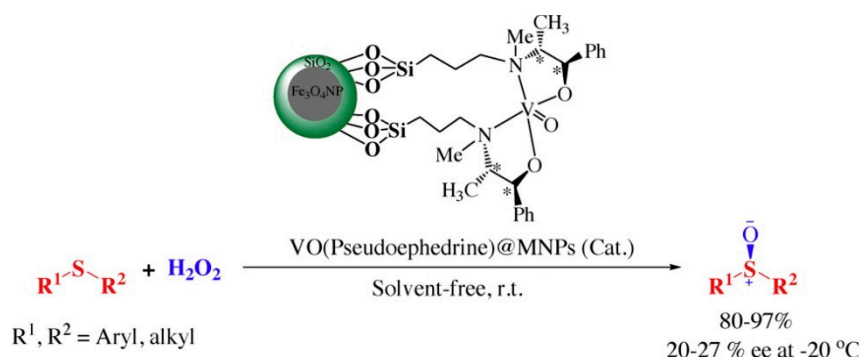
Figure 4. Chemoselective oxidation of sulfides to sulfoxides by means of VO(pseudoephedrine)-functionalized MNPs. Reprinted with permission from [56], Copyright Elsevier, 2015.

The same VO (pseudoephedrine)@MNPs catalyst was also able to catalyze, again at room temperature and under solvent-free conditions, the cyanosilylation of carbonyl compounds using trimethylsilyl cyanide with 8–25% enantiomeric excesses. Again, the catalyst was reused up to 15 times with minimal loss of activity and enantioselectivity [57].

Chiral proline-based polymeric nanoparticles were able to catalyze asymmetric aldol reaction both in organic and aqueous solvents [58]. The NPs, prepared by miniemulsion polymerization and with an average diameter of 160 nm, possessed high surface area, and the whole particle, not just the surface, was shown to be chiral. Although the enantioselectivity obtained with the nanoparticle catalyst was lower than that obtained with the free amino acid, the NPs have the advantage of being easily recovered and recycled. Moreover, this approach could be used to prepare a variety of polymeric NPs with different sizes, architectures, and chemical functionalities as new nanotechnology-based organocatalysts.

The same type of reaction, as well others, has been shown to be influenced by chiral amines and their byproducts. Silica-coated Fe_3O_4 MNPs were also functionalized with chiral bis-amine organocatalysts, such as glutamate, Pro-Glu dipeptide, or cyclohexyl-1,2-diamine, for catalyzing asymmetric aldol reaction [59]. Among the investigated amines, the NPs functionalized with the stiff cyclohexyl-1,2-diamine gave the best yield (up to 08%) and enantioselectivity (up to 96%), also showing good recyclability by keeping these values high even after three cycles (Figure 5).
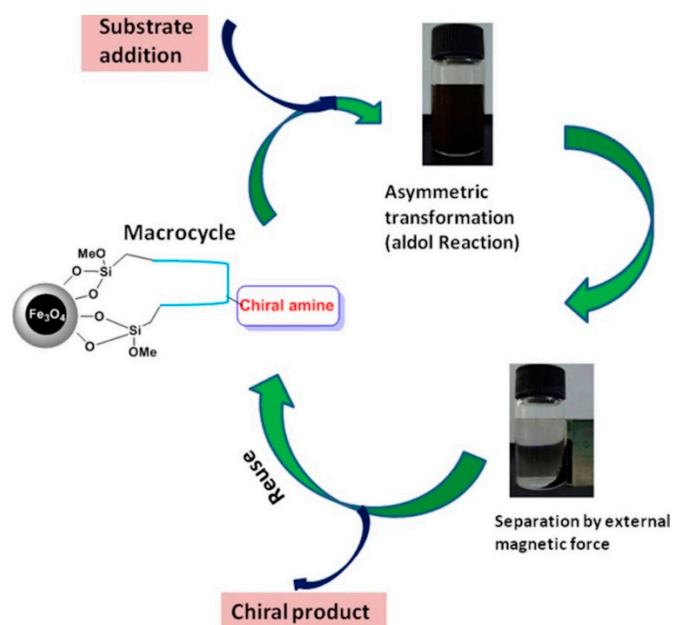
Figure 5. Mechanism of purification of asymmetric aldol reaction products by means of chiral MNPs. Reprinted with permission from [59], Copyright Elsevier, 2019.

In an alternative approach, chiral silica NPs loaded with (*P*)-1,12-dimethyl-8-methoxycarbonyl benzo[*c*]phenantrene were able to selectively adsorb, collect, and precipitate a diol disulfide from solution favoring its reaction with the rhodium catalyst in solution among other disulfides [60]. The diol disulfide was then removed from solution by precipitation, thus favoring an equilibrium shift in solution. This technique was successfully applied to racemic diol/diamine disulfides, and optically active diol disulfides were obtained in higher yields than those obtained by equilibrium without using the NPs.

Scrimin et al. developed catalytic NPs with behavior similar to that of natural enzymes and called them nanozymes [62]. For example, they exploited Au NPs as a platform for attaching thiols containing chiral Zn^{II}-binding head groups [61]. The resulting NPs presented chiral bimetallic catalytic sites that exhibited different hydrolytic activities for the enantiomers of a pure RNA model substrate. Thanks to the NPs' multivalency, substrate selectivity in the cleavage of UpU, GpG, ApA, and CpC and enantioselectivity in the cleavage of UpU were improved by exploiting additional binding interactions with the dinucleotides.

2.3. Biomedicine

Chirality is ubiquitous in nature and plays many essential roles in biological processes through homochirality of its basic constituents, i.e., L-amino acids and D-sugars. As a consequence, many chiral biomaterials have been prepared and their influence on biological systems investigated [63]. Chiral NPs have also been shown to possess different behaviors when interacting with biological systems, with the main findings of these studies being summarized in Table 3.

Table 3. Main applications of chiral NPs for biomedicine and their principal characteristics.

NPs	Surface Functionalization	Application	Reference
Se	Ru(II)-L-arginine	siRNA delivery	[64]
SiO$_2$	3-*N*-aminopropyl-L-tartaric acid	doxorubicin delivery	[65]
Ag@Au	aptamers	tumor targeting	[66]
PNBC polypeptides	-	camptothecin delivery	[67]
PMO	poly-L-lysine	drug delivery	[68]
Se	D-penicillamine	Aβ fibrillogenesis inhibition	[69]
Au	*N*-isobutyl-L-cysteine	amylin fibrillation inhibition	[70]
Au NCs and NOs	polyacryloyl-L-valine	cellular uptake/cytotoxicity	[71]
Ag	(*R*)-imazethapyr	cellular uptake/cytotoxicity	[72]
Ag	cysteine	cellular uptake/cytotoxicity	[73]
SiO$_2$	*N*-palmityl-L-alanine	indomethacin delivery	[74]
SiO$_2$	D-tartaric acid	indomethacin delivery	[75]
SiO$_2$	L-tartaric acid	indomethacin delivery	[76]
SiO$_2$	*N*-myristyl-L(D)-alanine	ibuprofen delivery	[77]
CdS	L-cysteine	BSA binding	[78]

For example, selenium nanoparticles stabilized with arginine (L(D)-Arg@Se NPs) and additionally functionalized with a dinuclear ruthenium (II) complex, acting as gene carrier and anti-tumor drug, were employed to efficiently deliver short interfering RNA (siRNA) that targeted the multi-drug resistance-1 (MDR1) gene [64]. Remarkably, Ru-L-Arg@Se NPs revealed high tumor-targeted fluorescence, improved anti-tumor efficacy, and reduced systemic toxicity compared to the D-Arg-capped NPs, both in vitro and in vivo.

Chiral interactions also allow for the obtaining of a more significant delivery of APIs. Mesoporous silica nanoparticles capped with 3-*N*-aminopropyl-L-tartaric acid were shown to be more effective in delivering doxorubicin compared to the corresponding achiral NPs, thus resulting in being more cytotoxic to MCF-7 cells [65].

Chiral interaction with biological systems was investigated by Zhao and colleagues who synthesized aptamer-driven chiral Ag@Au core shell nanoparticle assemblies that displayed marked

and opposite chiral bisignate plasmonic peaks [66]. The authors showed that the chiral assemblies were able to discriminate circulating HER2 tumor cells from normal cells. Similarly, Liu and colleagues showed that the chirality of poly(*S*-(*o*-nitrobenzyl)-L(D)-cysteine) (PNBC) polypeptides influenced their secondary structure and, as a further consequence, also the drug release and biological properties of the associated nanoparticles [67].

Kehr et al. also exploited the chirality-dependent cellular uptake of mesoporous silica nanoparticles (MSNs) but they showed that it can be influenced by the amount of organic molecules carried and by the chiral polymers covering periodic mesoporous organosilica (PMO) NPs [68]. As a result, the following release of different quantities of organic molecules to primary fibroblast cells also varied and the authors concluded that this behavior was caused and dominated by the formation of protein corona on the PMO surfaces.

A characteristic of Alzheimer's disease (AD) is the misfolding of amyloid-β (Aβ) into fibrils and its accumulation into plaques [79]. Consequently, one of the approaches for the treatment of this pathology is to inhibit Aβ fibrillogenesis. With this aim, Sun et al. prepared chiral penicillamine-capped selenium (L(D)-Pen@Se) NPs that could perform as Aβ inhibitors [69]. They observed that D-Pen@Se NPs were more efficient inhibitors and they improved both understanding and memory impairments. Furthermore, D-Pen@Se NPs also decreased Zn^{2+}-induced intracellular $Aβ_{40}$ fibrillation in PC12 cells, while L-Pen@Se NPs did not, suggesting a potential biomedical application of chiral D-Pen@Se NPs (Figure 6).
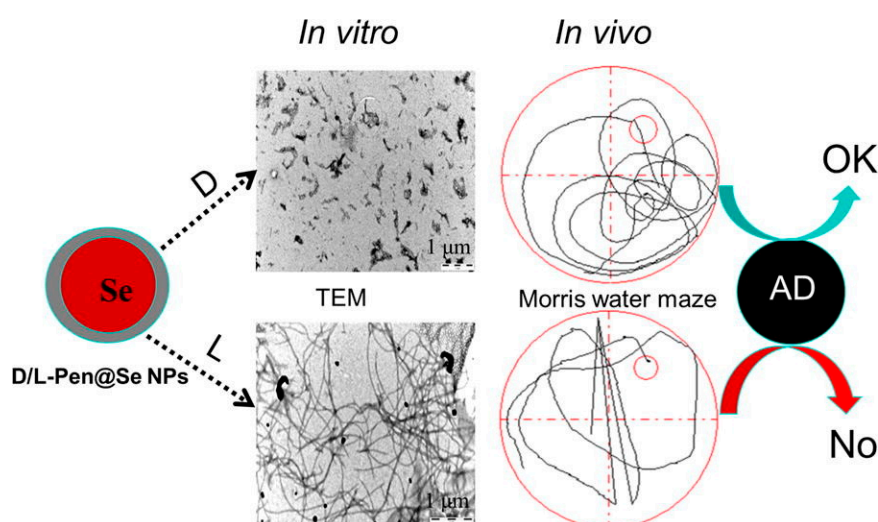
Figure 6. Inhibition effects of chiral penicillamine-capped NPs both in vitro and in vivo. Reprinted with permission from [69], Copyright Elsevier, 2017.

Li et al. used Au NPs (diameter of ≈4 nm) functionalized with *N*-isobutyl-L(D)-cysteine (L(D)-NIBC) as a prototype to exemplify the chiral effect on the amylin fibrillation at nano–bio interface [70]. The authors stated that both enantiomers were able to inhibit amylin fibrillation in a dose-dependent way but the inhibition obtained with the L-functionalized NPs was higher than that with the D-functionalized NPs. In situ real time CD spectra evidenced that L-NIBC-Au NPs were able to inhibit the conformational change of amylin from random coils to α-helix, while the D enantiomer could only delay but not avoid the construction of the α-helix. These encouraging results shed some light on the mechanism of formation of amyloid peptides from a chiral point of view and could help in designing novel therapeutic inhibitors for anti-amyloidosis formation in neurodegenerative diseases.

Chirality has also been shown to impact cellular internalization and cytotoxicity. Deng and colleagues reported that gold nanocubes (Au NCs) and nanooctahedras (Au NOs) covered with polyacryloyl-L(D)-valine (L(D)-PAV) exhibited different cytotoxicity to A549 cells despite having the same size, morphology, and ligand density [71]. The L-PAV-capped Au NCs and Au NOs exhibited

higher cytotoxicity than the D-PAV coated forms, and the PAV-Au NOs were more cytotoxic than PAV-Au NCs when capped with the same type of enantiomers, respectively. Their cytotoxicity was associated with the internalized amount and the subsequent production of intracellular reactive oxygen species (ROS).

Silver NPs, well known for their antibacterial activity, were functionalized with chiral molecules. For example, Wen and colleagues conjugated the herbicide imazethapyr (IM), usually employed as racemic mixture although just the (*R*) enantiomer is active, to Ag NPs and investigated their cytotoxic effect on *Arabidopsis thaliana* [72]. They showed that exposure of IM-Ag NPs to *A. thaliana* could intensify the enantioselective ecotoxicity. They found that the silver effectiveness in roots was 1.40-fold higher when bound to the herbicidally active (*R*)-IM than when capped to the (*S*) enantiomer. Similarly, Ag^+ concentration was 77.78% higher in sprouts when (*R*)-IM-Ag NPs were used instead of (*S*)-IM ones, suggesting a preferential uptake of the silver when bound to the (R) enantiomer.

Silver toxicity in chiral nanoparticles was also studied by Chen and colleagues, who functionalized them with cysteine and investigated their enantioselective phytotoxic effect [73]. Freshwater microalgae *Scenedesmus obliquus* and terrestrial plant *Arabidopsis thaliana* were used as a model and they behaved differently to exposure to the chiral system. The authors observed that Ag NPs exerted their toxicity to *S. obliquus* by exploiting Ag^+, produced in higher quantities by D-Cys-Ag NPs; on the other hand, *A. thaliana* was more susceptible to L-Cys-Ag NPs, which produced more ROS and oxidative stress.

Wang et al. exploited mesoporous silica nano-cocoons (A-CMSNs) functionalized with a chiral anionic surfactant, *N*-palmityl-L-alanine, for the drug delivery of indomethacin (IMC), a poorly water-soluble drug [74]. The use of chiral surfactants influenced the 2D hexagonal morphology of the A-CMSN with curled channels on its surface, differently from typical 2D hexagonal mesoporous silica nanoparticles with straightaway channels, thus also enhancing the drug loading and its release profile.

Zhou and colleagues also investigated the chiral recognition and subsequent release of IMC by two using concealed-body chiral mesoporous silica nanoparticles (Cb-L(D)-MSNs) prepared with either L- or D-tartaric acid [75]. Both Cb-D-MSN and Cb-L-MSN significantly improved IMC dissolution, oral bioavailability, and anti-inflammatory effects compared to achiral MSN and, even more interestingly, the two chiral MSNs showed different chiral recognition behavior, with the Cb-D-MSNs showing higher affinity for the drug and sodium-dependent glucose transporter (SLGT) (Figure 7).
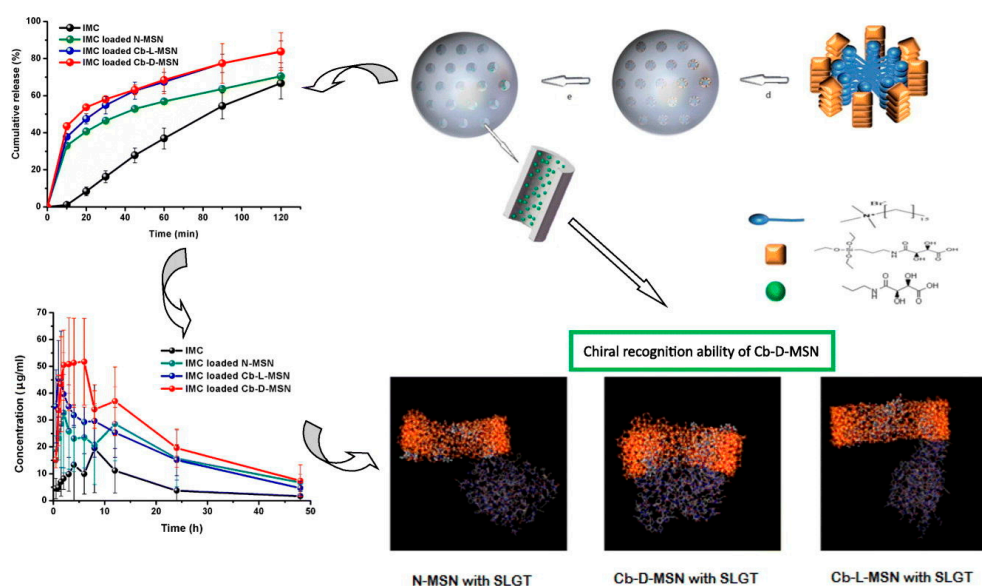
Figure 7. Enantioselective recognition and release of indomethacin (IMC) by means of concealed-body chiral MSNs prepared with either L- or D-tartaric acid. Reprinted with permission from [75], Copyright Elsevier, 2018.

Similar results were obtained by Fan et al. with on–off chiral mesoporous silica nanoparticles (On-Off-D-CMSN and On-Off-L-CMSN) [76]. The two IMC-loaded On-Off-L(D)-CMSNs exerted different chiral recognition functions with on–off mechanism in an in vitro chiral environment; however, this time the L enantiomer yielded a higher anti-inflammatory effect than the D enantiomer, probably because the NPs could trigger chirality of the biological environment, thus achieving on or off chiral recognition functions.

In order to investigate different geometries, twisted rod-like chiral MSNs were employed for solubilizing ibuprofen by using L- and D-alanine derivatives as templates to obtain chiral helical structures [77]. MSNs with different chirality were able to effectively encapsulate the drug, with the D enantiomer being more efficient, as well as being able to achieve drug release differentiation and enhance the dissolution of ibuprofen in simulated gastric fluid, depending on the pH of the medium and on the pore size of the MSNs.

Despite using a different metallic core, Yang et al. synthetized CdS NPs in anodic aluminum oxide (AAO) nanochannels and functionalized their surface with cysteine for binding BSA. They noted that the L enantiomer was able to bind more strongly the protein, thus enhancing the response sensitivity of BSA transport [78].

2.4. Biosensors

Chiral NPs and their nanocomposites have been shown to possess countless capabilities as tools for fabricating functional materials, such as non-linear optics and biological sensors and detectors [80]. The main findings about their exploitation as chiral biosensors are summarized in Table 4.

Table 4. Main applications of chiral NPs as biosensors and their principal characteristics.

NPs	Surface Functionalization	Molecule Detected	Reference
ZnO	L-cysteine	dopamine	[81]
Au	hemoglobin	D-penicillamine	[82]
Au	-	L(D)-triptophan	[83]
Poly(vinyl chloride)	-	*S*-citalopram	[84]
Au	-	*S*-citalopram	[85]
Au	-	L-alanine	[86]
Au@CoFe$_2$O$_4$	β-cyclodextrin	L(D)-triptophan	[87]
Ag	chitosan	L(D)-triptophan	[88]
Ag	-	D-cysteine	[89]
Au	mAb	tropomyosin	[90]
Au	-	L-Leu	[91]
Au	cysteine	L(D)-Tyr, L(D)-Trp, L(D)-Glu	[92]
Ag	(*R*)-mandelic acid-derived calix[4]arene	*N*-Fmoc-L(D)-aspartic acid	[93]
Au	L-tartaric cid	L(D)-mandelic acid	[94]

For example, ZnO NPs functionalized with L-cysteine were used for detecting dopamine in urine samples with high selectivity and sensitivity [81]. The system exploited the variation in photoluminescence of the chiral NPs that was quenched upon binding to the neurotransmitter.

On the other hand, a stereoselective electrochemiluminescence (ECL) interface was prepared for quantifying Pen enantiomers by using hemoglobin (Hb) and Au NP-functionalized graphite-like carbon nitride nanosheet composite attached to glassy carbon electrodes (Hb/Au-g-C$_3$N$_4$/GCE) [82]. Different ECL peaks were recorded from Pen enantiomers on the chiral interface although a larger response was obtained from the D-Pen derivatives, with a limit of detection of 3.3×10^{-5} M. As a proof of principle, this stereoselectivity was also exploited for measuring D-Pen in spiked tablet samples.

Surprisingly, Zhang et al. discovered that unmodified citrate-capped Au NPs (about 13 nm in diameter) could display chiral-selective response upon addition of L(D)-Trp [83]. However, a considerable red-to-blue color change of the gold solution could be detected in the presence

of D-Trp, while no color variation was observed when L-Trp was added. This process was used to quantify D-Trp in the range of 0.2–10 µM, with a remarkable limit of detection of 0.1 µM. Furthermore, the Au NPs could selectively adsorb D-Trp on their surface, and gentle centrifugation allowed the precipitation of D-Trp-bound Au NPs, while leaving in solution the other enantiomer, thus allowing separation of the racemate (Figure 8).
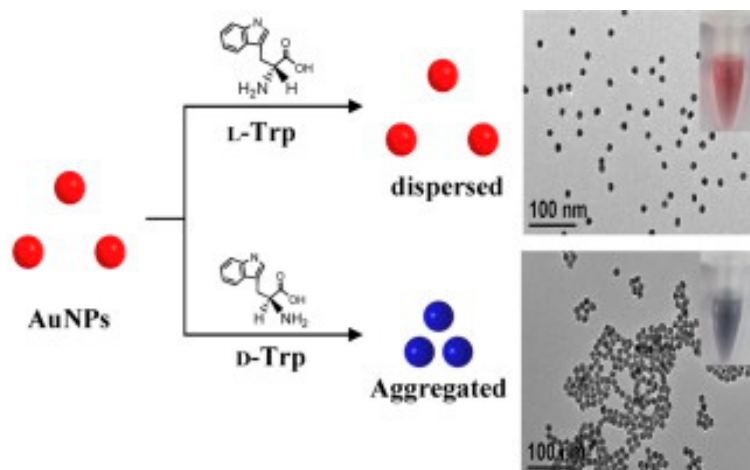
Figure 8. TEM images of the effect of Trp addition to a solution of citrate-capped Au NPs. Reprinted with permission from [83], Copyright Elsevier, 2014.

Barrio et al. exploited molecularly imprinted chiral polymeric particles to create a novel enantioselective sensor able to recognize *S*-citalopram, an antidepressant drug, used as a template in the synthetic step [84]. The sensor was able of precisely quantify *S*-citalopram in urine samples with a linear range and with very short response time in the interval range of concentration of clinically administered drug.

Citalopram was also detected by Tashkhourian and colleagues by using citrate-capped Au NPs, reporting a simple and reliable colorimetric method for the quantification of its enantiomers in aqueous solution, with detection limits of 2.1 µM [85]. *S*-citalopram, but not the other enantiomer, induced the aggregation of the Au NPs, probably because of electrostatic interactions and hydrogen bonding between the host and the guest, thus causing a reduction of the plasmon absorption peak at 520 nm and the development of a widened surface plasmon band around 600–700 nm. The method was effectively employed for the determination of citalopram in commercially available tablets, showing good precision and accuracy.

The colorimetric quantification of L-alanine in human serum was investigated by Zor and Bekar, who used inherently chiral Au NPs (about 8 nm in diameter) embedded in a paper-based lab-in-a-syringe device [86]. The device was based on the enantioselective recognition of the amino acid and the subsequent precipitation of the aggregate. The variation of the color of the solution allowed for the determination of alanine with a limit of detection of 0.77 mM.

Munoz et al. presented a novel, facile, and generic procedure that exploited the electrocatalytic properties of chiral magnetic nanobiofluids (mNBFs) and the electrochemical enantiobiosensing ability of a magneto nanocomposite graphene paste electrode (mNC–GPE) [87]. A specific chiral mNBF, based on an aqueous dispersion of cobalt ferrite loaded with β-cyclodextrin coated Au NPs (β–CD-Au@CoFe$_2$O$_4$ NPs), was exploited for the enantioselective recognition of tryptophan, although the procedure could be easily adapted to many other APIs, thus opening up new approaches for enantio(bio)sensing. Tryptophan was also determined by a novel, fast, and economical sensor by using chitosan-capped Ag NPs [88]. The sensor was based on the colorimetric measurement by scanometry and spectrophotometry of a reaction solution comprising chitosan-capped Ag NPs, phosphate buffer, and tryptophan.

A recent colorimetric sensing platform for the enantioselective recognition of chiral analytes also exploited Ag NPs that were embedded into translucent nanopaper [89]. The nanopaper was prepared by an environmentally friendly method that exploited bacterial cellulose made of nanofibers while the Ag NPs were synthesized in situ, thus allowing their direct encapsulation. The NPs presented a selective sensing reply toward D-cysteine with a limit of detection of 4.88 µM (Figure 9).
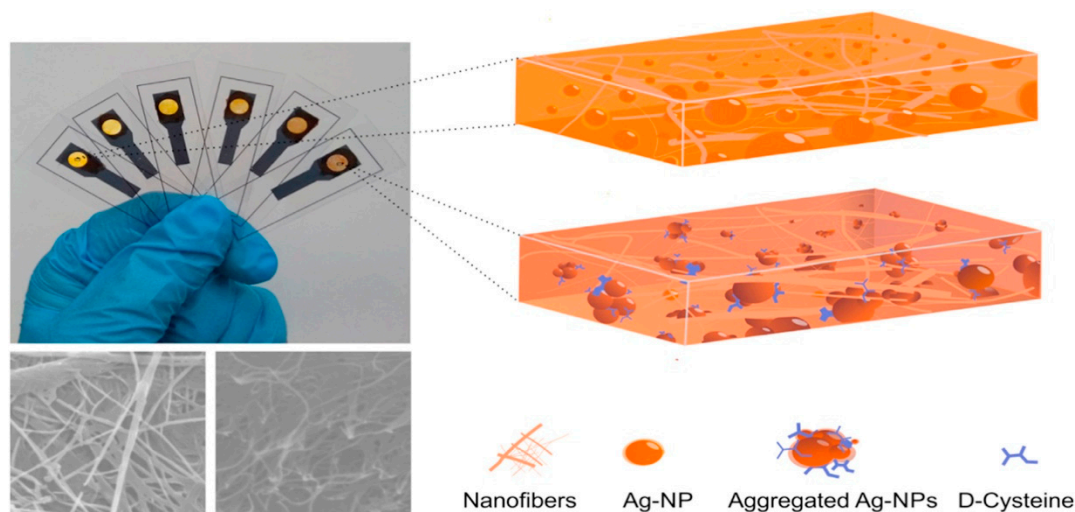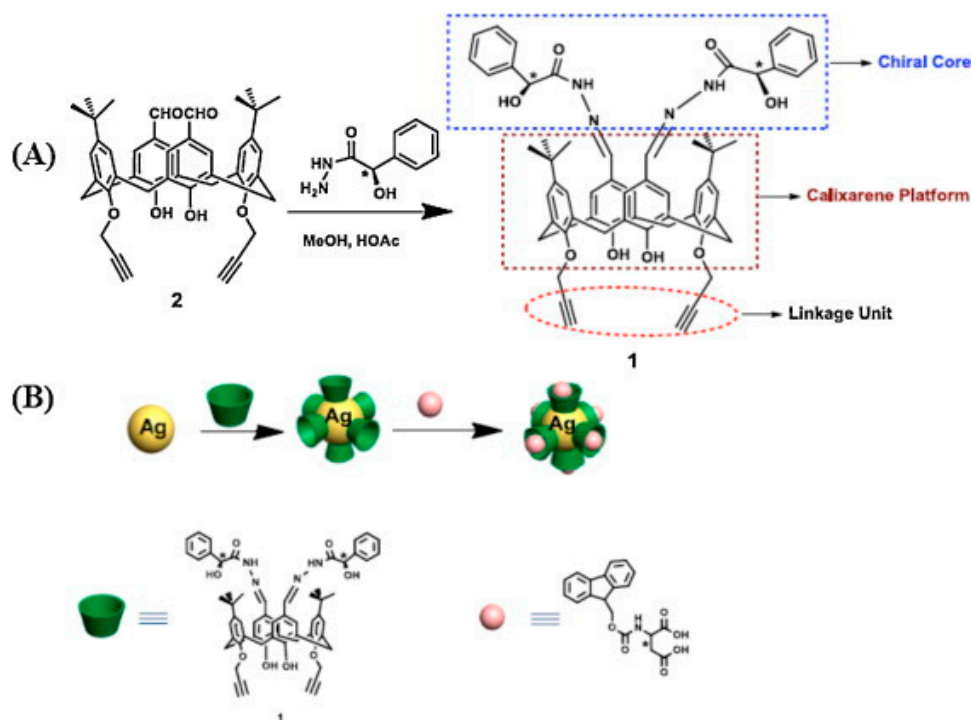

Figure 9. Schematic representation of the chiral nanopaper for the colorimetric determination of D-cysteine. Reprinted with permission from [89], Copyright Elsevier, 2018.

A biosensor based on chiral assemblies of Au NP coupled with CD spectroscopy was developed for the recognition and quantification of tropomyosin (TROP), considered to be the major allergen in shellfish allergy [90]. Monoclonal antibody-Au NP and TROP-Au NP probes could organize into terpolymers or aggregates of diverse oligomers, depending on the concentration of the free antigen. The biosensor was able to quantify the allergen in seven different shellfish species, with good repeatability and accuracy, remarkable specificity, and an impressive limit of detection of 21 nM.

A similar approach, but with cube-shaped gold nanoparticles, was employed for the determination of leucine [91]. The colorimetric analysis exploited the ability of L-Leu, but not D-Leu, to induce rapid aggregation of Au NCs (average edge of about 46 nm), thus causing a color variation of the solution from red to transparent, yielding a modest, cheap, quick, and easy-to-function sensing system. Interestingly, the enantioselectivity was associated with the geometrical structure of the NPs because only the NCs, but not similar spherical or rod-shaped Au nanocrystals, were able to discriminate the amino acid.

Zhang et al. successfully fabricated a device measuring both potential difference and current ratio that exploited left/right-handed double helix carbon nanotubes functionalized with polypyrrole-containing cysteine-capped Au NPs (L(D)-DHCNT@PPy@L(D)-Cys-Au) via a facile and environmentally friendly procedure [92]. This highly efficient electrochemical chiral sensor exploited the chiral structure of L(D)-Cys and L(D)-DHCNT, and the exceptional conductivity of PPy and Au NPs, thus being able to distinguish and quantify tyrosine (Tyr), tryptophan (Trp), and glutamic acid (Glu) enantiomers.

By covering Ag NPs with a chiral (*R*)-mandelic acid-derived calix[4]arene, Sun et al. managed to quantify *N*-Fmoc-L(D)-aspartic acid in solution by measuring through dynamic light scattering (DLS) the assemblies formed with the NPs (Figure 10) [93]. With this technique, the detection sensitivity was enhanced by almost 500-fold compared to that obtained via the traditional Ag NP method, reaching a detection limit of 50 nM.

Figure 10. (**A**) Synthetic scheme of the preparation of the *R*-mandelic acid-functionalized calix[4]arene and (**B**) schematic representation of Ag NPs coated with the calix[4]arene derivative for detecting *N*-Fmoc-D/L-aspartic acid. Reprinted with permission from [93], Copyright Elsevier, 2015.

On the other hand, Song et al. described a process for the colorimetric determination of L- and D-mandelic acid (MA) [94]. Their method was built on the chirality of L-tartaric acid-functionalized Au NPs (about 13 nm in diameter) that could be exploited as selectors for either enantiomers of MA. When L-MA was added to a solution containing the L-TA-capped Au NPs, the researchers observed a color variation from red to blue; however, no color transition was noted when D-MA was added, yielding a simple and cheap technique compared to common chiral recognition procedures, such as gas chromatography, HPLC, circular dichroism, and nuclear magnetic resonance (NMR), yet with good sensitivity.

3. Conclusions

Chirality is at the base of nature and natural phenomena. Similarly, chiral molecules are fundamental in many chemical and biological synthetic processes. APIs often contain at least one chiral center, however, only one enantiomer possess beneficial pharmacological effects, while the other is not active or even toxic. As a consequence, racemic mixtures need to be separated, requiring costly additional steps. In alternative, the development of methodologies that can provide only one single enantiomer over another should be preferred, thus directly yielding the enantiomer of interest.

Nanotechnology has made huge steps over the last decades and its influence is also gaining increasing importance in chiral applications. Metallic nanoparticles, such as gold and silver NPs; magnetic nanoparticles; and fluorescent quantum rods have already been exploited in a variety of fields, such as biosensing and biomedicine, demonstrating their potential. In this regard, preparation and functionalization of chiral NPs can extend their exploitability to additional fields or improve the applicability of already explored fields.

In this review, we analyzed recent applications of chiral nanoparticles in four major research fields, such as enantioselective recognition, asymmetric catalysis, biomedicine, and biosensing. These fields have attracted much attention because of their importance and potential. Despite the fact that much progress can be still made in order to optimize these novel tools, nanotechnology has already been

shown to be able to overcome the limitations of traditional approaches. For example, combination of NPs with enantioselective recognition can improve separation ability of HPLC systems, as well as enhance sensitivity and detection limits of novel chiral biosensors. Chiral recognition can also induce specific interactions with chiral receptors on the surface of cells, thus improving internalization and/or cytotoxicity.

Many improvements can be still made, and novel approaches must be investigated to make a step forward. We believe that enantioselectivity will gain even more importance in the future of nanotechnology and we hope that the articles reported in this review will help to stimulate new ideas and designs.

Author Contributions: Writing—original draft preparation, M.S.Z.; writing—review and editing, A.R. All authors have read and agreed to the published version of the manuscript.

Conflicts of Interest: The authors declare no conflict of interest.

References

1. Guo, P.; Driver, D.; Zhao, Z.; Zheng, Z.; Chan, C.; Cheng, X. Controlling the Revolving and Rotating Motion Direction of Asymmetric Hexameric Nanomotor by Arginine Finger and Channel Chirality. *ACS Nano* **2019**, *13*, 6207–6223. [CrossRef]
2. Wattanakit, C.; Côme, Y.B.S.; Lapeyre, V.; Bopp, P.A.; Heim, M.; Yadnum, S.; Nokbin, S.; Warakulwit, C.; Limtrakul, J.; Kuhn, A. Enantioselective recognition at mesoporous chiral metal surfaces. *Nat. Commun.* **2014**, *5*, 3325. [CrossRef]
3. Xie, J.; Duan, Y.; Che, S. Chirality of Metal Nanoparticles in Chiral Mesoporous Silica. *Adv. Funct. Mater.* **2012**, *22*, 3784–3792. [CrossRef]
4. Zor, E.; Bingol, H.; Ramanaviciene, A.; Ramanavicius, A.; Ersoz, M. An electrochemical and computational study for discrimination of d- and l-cystine by reduced graphene oxide/β-cyclodextrin. *Analyst* **2015**, *140*, 313–321. [CrossRef]
5. Vogel, G. How Does a Single Somatic Cell Become a Whole Plant? *Science* **2005**, *309*, 86. [CrossRef]
6. He, M.; Fedotov, P.; Chernov, A.; Obraztsova, E.D.; Jiang, H.; Wei, N.; Cui, H.; Sainio, J.; Zhang, W.; Jin, H.; et al. Chiral-selective growth of single-walled carbon nanotubes on Fe-based catalysts using CO as carbon source. *Carbon* **2016**, *108*, 521–528. [CrossRef]
7. Wang, X.; Li, M.; Song, P.; Lv, X.; Liu, Z.; Huang, J.; Yan, Y. Reversible Manipulation of Supramolecular Chirality using Host-Guest Dynamics between β-Cyclodextrin and Alkyl Amines. *Chem. A Eur. J.* **2018**, *24*, 13734–13739. [CrossRef]
8. Tan, C.; Qi, X.; Liu, Z.; Zhao, F.; Li, H.; Huang, X.; Shi, L.; Zheng, B.; Xie, L.; Tang, Z.; et al. Self-Assembled Chiral Nanofibers from Ultrathin Low-Dimensional Nanomaterials. *J. Am. Chem. Soc.* **2015**, *137*, 1565–1571. [CrossRef]
9. Biedermann, F.; Nau, W.M. Noncovalent Chirality Sensing Ensembles for the Detection and Reaction Monitoring of Amino Acids, Peptides, Proteins, and Aromatic Drugs. *Angew. Chem. Int. Ed.* **2014**, *53*, 5694–5699. [CrossRef]
10. Caner, H.; Groner, E.; Levy, L.; Agranat, I. Trends in the development of chiral drugs. *Drug Discov. Today* **2004**, *9*, 105–110. [CrossRef]
11. Lanone, S.; Boczkowski, J. Biomedical applications and potential health risks of nanomaterials: Molecular mechanisms. *Curr. Mol. Med.* **2006**, *6*, 651–663. [CrossRef]
12. Xu, L.; Li, X.; Ma, J.; Wen, Y.; Liu, W. Nano-MnO x on activated carbon prepared by hydrothermal process for fast and highly efficient degradation of azo dyes. *Appl. Catal. A Gen.* **2014**, *485*, 91–98. [CrossRef]
13. Li, X.; Liu, W.; Ma, J.; Wen, Y.; Wu, Z. High catalytic activity of magnetic FeO /NiO /SBA-15: The role of Ni in the bimetallic oxides at the nanometer level. *Appl. Catal. B Environ.* **2015**, *179*, 239–248. [CrossRef]
14. Liu, W.; Ma, J.; Shen, C.; Wen, Y.; Liu, W. A pH-responsive and magnetically separable dynamic system for efficient removal of highly dilute antibiotics in water. *Water Res.* **2016**, *90*, 24–33. [CrossRef]

15. Harris, K.D.M.; Thomas, S.J.M. Selected Thoughts on Chiral Crystals, Chiral Surfaces, and Asymmetric Heterogeneous Catalysis. *ChemCatChem* **2009**, *1*, 223–231. [CrossRef]

16. Verbiest, T. Strong Enhancement of Nonlinear Optical Properties Through Supramolecular Chirality. *Science* **1998**, *282*, 913–915. [CrossRef]

17. Jadzinsky, P.D.; Calero, G.; Ackerson, C.J.; Bushnell, D.A.; Kornberg, R.D. Structure of a Thiol Monolayer-Protected Gold Nanoparticle at 1.1 A Resolution. *Science* **2007**, *318*, 430–433. [CrossRef]

18. Schneider, H.-J.; Yatsimirsky, A.K. Selectivity in supramolecular host–guest complexes. *Chem. Soc. Rev.* **2008**, *37*, 263–277. [CrossRef]

19. Ragusa, A.; Rossi, S.; Hayes, J.M.; Stein, M.; Kilburn, J.D. Novel Enantioselective Receptors for N-Protected Glutamate and Aspartate. *Chem. A Eur. J.* **2005**, *11*, 5674–5688. [CrossRef]

20. Khose, V.N.; John, M.E.; Pandey, A.D.; Borovkov, V.V.; Karnik, A.V. Chiral Heterocycle-Based Receptors for Enantioselective Recognition. *Symmetry* **2018**, *10*, 34. [CrossRef]

21. Ragusa, A.; Hayes, J.M.; Light, M.E.; Kilburn, J.D. Predicting Enantioselectivity: Computation as an Efficient "Experimental" Tool for Probing Enantioselectivity. *Eur. J. Org. Chem.* **2006**, *2006*, 3545–3549. [CrossRef]

22. Ragusa, A.; Hayes, J.M.; Light, M.E.; Kilburn, J.D. A Combined Computational and Experimental Approach for the Analysis of the Enantioselective Potential of a New Macrocyclic Receptor for N-Protected α-Amino Acids. *Chem. A Eur. J.* **2007**, *13*, 2717–2728. [CrossRef]

23. Shukla, N.; Ondeck, N.; Gellman, A.J. Quantitation of enantiospecific adsorption on chiral nanoparticles from optical rotation. *Surf. Sci.* **2014**, *629*, 15–19. [CrossRef]

24. Shukla, N.; Yang, D.; Gellman, A.J. Enantiomeric separations of chiral pharmaceuticals using chirally modified tetrahexahedral Au nanoparticles. *Surf. Sci.* **2016**, *648*, 29–34. [CrossRef]

25. Ghosh, S.; Badruddoza, A.Z.M.; Uddin, M.S.; Hidajat, K. Adsorption of chiral aromatic amino acids onto carboxymethyl-β-cyclodextrin bonded Fe3O4/SiO2 core—Shell nanoparticles. *J. Colloid Interface Sci.* **2011**, *354*, 483–492. [CrossRef]

26. Ghosh, S.; Fang, T.H.; Uddin, M.; Hidajat, K. Enantioselective separation of chiral aromatic amino acids with surface functionalized magnetic nanoparticles. *Colloids Surf. B Biointerfaces* **2013**, *105*, 267–277. [CrossRef]

27. Li, Y.-Y.; Wei, M.; Chen, T.; Zhu, N.; Ma, Y. Self-assembled cyclodextrin-modified gold nanoparticles on silica beads as stationary phase for chiral liquid chromatography and hydrophilic interaction chromatography. *Talanta* **2016**, *160*, 72–78. [CrossRef]

28. Fu, Y.; Huang, T.; Chen, B.; Shen, J.; Duan, X.; Zhang, J.; Li, W. Enantioselective resolution of chiral drugs using BSA functionalized magnetic nanoparticles. *Sep. Purif. Technol.* **2013**, *107*, 11–18. [CrossRef]

29. Wu, J.; Su, P.; Huang, J.; Wang, S.; Yang, Y. Synthesis of teicoplanin-modified hybrid magnetic mesoporous silica nanoparticles and their application in chiral separation of racemic compounds. *J. Colloid Interface Sci.* **2013**, *399*, 107–114. [CrossRef]

30. Fang, L.-L.; Wang, P.; Wen, X.-L.; Guo, X.; Luo, L.-D.; Yu, J.; Guo, X. Layer-by-layer self-assembly of gold nanoparticles/thiols β-cyclodextrin coating as the stationary phase for enhanced chiral differentiation in open tubular capillary electrochromatography. *Talanta* **2017**, *167*, 158–165. [CrossRef]

31. Lu, J.E.; Peng, Y.; Chen, S. Janus Nanoparticle Emulsions as Chiral Nanoreactors for Enantiomerically Selective Ligand Exchange. *Part. Part. Syst. Charact.* **2019**, *36*, 1800564. [CrossRef]

32. Yang, L.; Kwan, C.; Zhang, L.; Li, X.; Han, Y.; Leung, K.C.-F.; Yang, Y.; Huang, Z. Chiral Nanoparticle-Induced Enantioselective Amplification of Molecular Optical Activity. *Adv. Funct. Mater.* **2018**, *29*, 1807307. [CrossRef]

33. Řezanka, P.; Záruba, K.; Král, V. Supramolecular chirality of cysteine modified silver nanoparticles. *Colloids Surf. A Physicochem. Eng. Asp.* **2011**, *374*, 77–83. [CrossRef]

34. Zhang, H.; Xin, X.; Sun, J.; Zhao, L.; Shen, J.; Song, Z.; Yuan, S. Self-assembled chiral helical nanofibers by amphiphilic dipeptide derived from d- or l-threonine and application as a template for the synthesis of Au and Ag nanoparticles. *J. Colloid Interface Sci.* **2016**, *484*, 97–106. [CrossRef]

35. Veiseh, O.; Sun, C.; Gunn, J.; Kohler, N.; Gabikian, P.; Lee, N.; Bhattarai, N.; Ellenbogen, R.; Sze, R.; Hallahan, A.; et al. Optical and MRI Multifunctional Nanoprobe for Targeting Gliomas. *Nano Lett.* **2005**, *5*, 1003–1008. [CrossRef]

36. Huh, Y.-M.; Jun, Y.-W.; Song, H.-T.; Kim, S.; Choi, J.-S.; Lee, J.-H.; Yoon, S.; Kim, K.-S.; Shin, J.-S.; Suh, J.-S.; et al. In Vivo Magnetic Resonance Detection of Cancer by Using Multifunctional Magnetic Nanocrystals. *J. Am. Chem. Soc.* **2005**, *127*, 12387–12391. [CrossRef]

37. Latham, A.H.; Tarpara, A.N.; Williams, M.E. Magnetic Field Switching of Nanoparticles between Orthogonal Microfluidic Channels. *Anal. Chem.* **2007**, *79*, 5746–5752. [CrossRef]

38. Pamme, N. Magnetism and microfluidics. *Lab Chip* **2006**, *6*, 24–38. [CrossRef]

39. Gijs, M.A.M. Magnetic bead handling on-chip: New opportunities for analytical applications. *Microfluid. Nanofluidics* **2004**, *1*, 22–40. [CrossRef]

40. Chiriacò, F.; Soloperto, G.; Greco, A.; Conversano, F.; Ragusa, A.; Menichetti, L.; Casciaro, S. Magnetically-coated silica nanospheres for dual-mode imaging at low ultrasound frequency. *World J. Radiol.* **2013**, *5*, 411–420. [CrossRef]

41. Quarta, A.; Amorín, M.; Aldegunde, M.J.; Blasi, L.; Ragusa, A.; Nitti, S.; Pugliese, G.; Gigli, G.; Granja, J.R.; Pellegrino, T. Novel synthesis of platinum complexes and their intracellular delivery to tumor cells by means of magnetic nanoparticles. *Nanoscale* **2019**, *11*, 23482–23497. [CrossRef] [PubMed]

42. Govorov, A.O.; Fan, Z.; Hernandez, P.; Slocik, J.M.; Naik, R.R. Theory of Circular Dichroism of Nanomaterials Comprising Chiral Molecules and Nanocrystals: Plasmon Enhancement, Dipole Interactions, and Dielectric Effects. *Nano Lett.* **2010**, *10*, 1374–1382. [CrossRef] [PubMed]

43. Knowles, W.S. Asymmetric hydrogenations (Nobel lecture). *Angew. Chem. Int. Ed.* **2002**, *41*, 1998–2007. [CrossRef]

44. Noyori, R. Asymmetric catalysis: Science and opportunities (Nobel lecture). *Angew. Chem. Int. Ed.* **2002**, *41*, 2008–2022. [CrossRef]

45. Orito, Y.; Imai, H.; Niwa, S. Asymmetric hydrogenation of methyl pyruvate with cinchonidine modified platinum-carbon catalyst. *J. Chem. Soc. Jap.* **1979**, *8*, 1118–1120.

46. Watson, D.; Jesudason, R.B.R.J.; Beaumont, S.K.; Kyriakou, G.; Burton, J.W.; Lambert, R.M. Heterogeneously Catalyzed Asymmetric Hydrogenation of C=C Bonds Directed by Surface-Tethered Chiral Modifiers. *J. Am. Chem. Soc.* **2009**, *131*, 14584–14589. [CrossRef] [PubMed]

47. Hutchings, G.J. HETEROGENEOUS ASYMMETRIC CATALYSTS: Strategies for Achieving High Enantioselection. *Annu. Rev. Mater. Res.* **2005**, *35*, 143–166. [CrossRef]

48. Blaser, H.-U.; Spindler, F.; Studer, M. Enantioselective catalysis in fine chemicals production. *Appl. Catal. A Gen.* **2001**, *221*, 119–143. [CrossRef]

49. Kyriakou, G.; Beaumont, S.K.; Lambert, R.M. Aspects of Heterogeneous Enantioselective Catalysis by Metals. *Langmuir* **2011**, *27*, 9687–9695. [CrossRef]

50. Barlow, S.; Raval, R. Complex organic molecules at metal surfaces: Bonding, organisation and chirality. *Surf. Sci. Rep.* **2003**, *50*, 201–341. [CrossRef]

51. Eralp, T.; Ievins, A.; Shavorskiy, A.; Jenkins, S.J.; Held, G. The Importance of Attractive Three-Point Interaction in Enantioselective Surface Chemistry: Stereospecific Adsorption of Serine on the Intrinsically Chiral Cu {531} Surface. *J. Am. Chem. Soc.* **2012**, *134*, 9615–9621. [CrossRef]

52. Yasukawa, T.; Miyamura, H.; Kobayashi, S. Chiral Ligand-Modified Metal Nanoparticles as Unique Catalysts for Asymmetric C–C Bond-Forming Reactions: How Are Active Species Generated? *ACS Catal.* **2016**, *6*, 7979–7988. [CrossRef]

53. Watson, D.; Acharya, S.; Nicklin, R.E.; Held, G. Observing the in situ chiral modification of Ni nanoparticles using scanning transmission X-ray microspectroscopy. *Surf. Sci.* **2014**, *629*, 108–113. [CrossRef]

54. Xue, X.; Chen, P.; Xu, P.; Wang, Y. Highly efficient and recyclable chiral Pt nanoparticle catalyst for enantioselective hydrogenation of activated ketones. *Catal. Commun.* **2018**, *110*, 55–58. [CrossRef]

55. Ng, E.-P.; Law, S.-P.; Mukti, R.R.; Juan, J.C.; Adam, F. Hydroamination of cyclohexene enhanced by ZnCl2 nanoparticles supported on chiral mesoporous silica. *Chem. Eng. J.* **2014**, *243*, 99–107. [CrossRef]

56. Rostami, A.; Atashkar, B. Chiral oxo-vanadium (+)-pseudoephedrine complex immobilized on magnetic nanoparticles: A highly efficient and recyclable novel nanocatalyst for the chemoselective oxidation of sulfides to sulfoxides using H2O2. *J. Mol. Catal. A Chem.* **2015**, *398*, 170–176. [CrossRef]

57. Rostami, A.; Atashkar, B. Synthesis, characterization and catalytic property of chiral oxo-vanadium (+)-pseudoephedrine complex supported on magnetic nanoparticles Fe3O4 in the cyanosilylation of carbonyl compounds. *Catal. Commun.* **2015**, *58*, 80–84. [CrossRef]

58. Adler, S.R.; Mastai, Y. Chiral polymeric nanoparticles for aldol reaction. *React. Funct. Polym.* **2015**, *96*, 1–4. [CrossRef]

59. Angamuthu, V.; Tai, D.-F. Chiral amine and macrocycle fabricated magnetic nanoparticle asymmetrically catalyzed direct aldol reaction. *Sustain. Chem. Pharm.* **2019**, *13*, 100152. [CrossRef]

60. Miyagawa, M.; Arisawa, M.; Yamaguchi, M. Equilibrium shift induced by chiral nanoparticle precipitation in rhodium-catalyzed disulfide exchange reaction. *Tetrahedron* **2015**, *71*, 4920–4926. [CrossRef]

61. Chen, J.L.Y.; Pezzato, C.; Scrimin, P.; Prins, L.J. Chiral Nanozymes—Gold Nanoparticle-based Transphosphorylation Catalysts Capable of Enantiomeric Discrimination. *Chem. A Eur. J.* **2016**, *22*, 7028–7032. [CrossRef]

62. Gabrielli, L.; Prins, L.J.; Rastrelli, F.; Mancin, F.; Scrimin, P. Hydrolytic Nanozymes. *Eur. J. Org. Chem.* **2020**. *early view*. [CrossRef]

63. Zhang, M.; Qing, G.; Sun, T. Chiral biointerface materials. *Chem. Soc. Rev.* **2012**, *41*, 1972–1984. [CrossRef]

64. Chen, Q.; Yu, Q.; Liu, Y.; Bhavsar, D.; Yang, L.; Ren, X.; Sun, N.; Zheng, W.; Liu, J.; Chen, L. Multifunctional selenium nanoparticles: Chiral selectivity of delivering MDR-siRNA for reversal of multidrug resistance and real-time biofluorescence imaging. *Nanomed. Nanotechnol. Boil. Med.* **2015**, *11*, 1773–1784. [CrossRef]

65. Li, J.; Du, X.; Zheng, N.; Xu, L.; Xu, J.; Li, S. Contribution of carboxyl modified chiral mesoporous silica nanoparticles in delivering doxorubicin hydrochloride in vitro: pH-response controlled release, enhanced drug cellular uptake and cytotoxicity. *Colloids Surf. B Biointerfaces* **2016**, *141*, 374–381. [CrossRef]

66. Zhao, Y.; Yang, Y.; Zhao, J.; Weng, P.; Pang, Q.; Song, Q. Dynamic Chiral Nanoparticle Assemblies and Specific Chiroplasmonic Analysis of Cancer Cells. *Adv. Mater.* **2016**, *28*, 4877–4883. [CrossRef]

67. Liu, Y.; Dong, C. Effect of chirality on conformation and cellular uptake of poly (S-(o-nitrobenzyl)-l,d-cysteine) polypeptides. *Chin. Chem. Lett.* **2017**, *28*, 827–831. [CrossRef]

68. Kehr, N.S.; Jose, J. Chirality-dependent cellular uptake of chiral nanocarriers and intracellular delivery of different amounts of guest molecules. *Appl. Surf. Sci.* **2017**, *425*, 432–439. [CrossRef]

69. Cook, N.P.; Archer, C.M.; Fawver, J.N.; Schall, H.E.; Rodriguez-Rivera, J.; Dineley, K.T.; Martí, A.A.; Murray, I. Ruthenium Red Colorimetric and Birefringent Staining of Amyloid-β Aggregates in Vitro and in Tg2576 Mice. *ACS Chem. Neurosci.* **2013**, *4*, 379–384. [CrossRef]

70. Sun, D.; Zhang, W.; Yu, Q.; Chen, X.; Xu, M.; Zhou, Y.; Liu, J. Chiral penicillamine-modified selenium nanoparticles enantioselectively inhibit metal-induced amyloid β aggregation for treating Alzheimer's disease. *J. Colloid Interface Sci.* **2017**, *505*, 1001–1010. [CrossRef]

71. Li, J.; Chen, R.; Zhang, S.; Ma, Z.; Luo, Z.; Gao, G. Chiral Effect at Nano-Bio Interface: A Model of Chiral Gold Nanoparticle on Amylin Fibrillation. *Nanomater* **2019**, *9*, 412. [CrossRef]

72. Deng, J.; Yao, M.; Gao, C. Cytotoxicity of gold nanoparticles with different structures and surface-anchored chiral polymers. *Acta Biomater.* **2017**, *53*, 610–618. [CrossRef]

73. Wen, Y.; Zhang, L.; Chen, Z.; Sheng, X.; Qiu, J.; Xu, D. Co-exposure of silver nanoparticles and chiral herbicide imazethapyr to Arabidopsis thaliana: Enantioselective effects. *Chemosphere* **2016**, *145*, 207–214. [CrossRef]

74. Chen, Z.; Sheng, X.; Wang, J.; Wen, Y. Silver nanoparticles or free silver ions work? An enantioselective phytotoxicity study with a chiral tool. *Sci. Total. Environ.* **2018**, *610*, 77–83. [CrossRef]

75. Wang, X.; Li, C.; Fan, N.; Li, J.; Zhang, H.; Shang, L.; He, Z.; Sun, J. Amino functionalized chiral mesoporous silica nanoparticles for improved loading and release of poorly water-soluble drug. *Asian J. Pharm. Sci.* **2018**, *14*, 405–412. [CrossRef]

76. Zhou, J.; Zhu, F.; Li, J.; Wang, Y. Concealed body mesoporous silica nanoparticles for orally delivering indometacin with chiral recognition function. *Mater. Sci. Eng. C* **2018**, *90*, 314–324. [CrossRef]

77. Fan, N.; Liu, R.; Ma, P.; Wang, X.; Li, C.; Li, J. The On-Off chiral mesoporous silica nanoparticles for delivering achiral drug in chiral environment. *Colloids Surf. B Biointerfaces* **2019**, *176*, 122–129. [CrossRef]

78. Wang, Y.; Li, W.; Liu, T.; Xu, L.; Guo, Y.; Ke, J.; Li, S.; Li, H. Design and preparation of mesoporous silica carriers with chiral structures for drug release differentiation. *Mater. Sci. Eng. C* **2019**, *103*, 109737. [CrossRef]

79. Yang, X.; Wang, T.; Zhang, H.; Chen, Q.; Wang, B.; Wang, Y.; Meng, D. Chiral cysteine selective transport of proteins by CdS nanostructures modified anodic aluminum oxide template. *J. Photochem. Photobiol. A Chem.* **2019**, *380*, 111830. [CrossRef]

80. Daniel, M.-C.; Astruc, D. Gold Nanoparticles: Assembly, Supramolecular Chemistry, Quantum-Size-Related Properties, and Applications toward Biology, Catalysis, and Nanotechnology. *Chem. Rev.* **2004**, *104*, 293–346. [CrossRef]

81. Lin, J.; Huang, B.; Dai, Y.; Wei, J.; Chen, Y. Chiral ZnO nanoparticles for detection of dopamine. *Mater. Sci. Eng. C* **2018**, *93*, 739–745. [CrossRef]

82. Lin, X.; Zhu, S.; Wang, Q.; Xia, Q.; Ran, P.; Fua, Y. Chiral recognition of penicillamine enantiomers using hemoglobin and gold nanoparticles functionalized graphite-like carbon nitride nanosheets via electrochemiluminescence. *Colloids Surf. B Biointerfaces* **2016**, *148*, 371–376. [CrossRef]

83. Zhang, L.; Xu, C.; Liu, C.; Li, B. Visual chiral recognition of tryptophan enantiomers using unmodified gold nanoparticles as colorimetric probes. *Anal. Chim. Acta* **2014**, *809*, 123–127. [CrossRef]

84. Gutiérrez-Climente, R.; Gómez-Caballero, A.; Unceta, N.; Goicolea, M.A.; Barrio, R.J. A new potentiometric sensor based on chiral imprinted nanoparticles for the discrimination of the enantiomers of the antidepressant citalopram. *Electrochim. Acta* **2016**, *196*, 496–504. [CrossRef]

85. Tashkhourian, J.; Afsharinejad, M.; Zolghadr, A.R. Colorimetric chiral discrimination and determination of S-citalopram based on induced aggregation of gold nanoparticles. *Sens. Actuators B Chem.* **2016**, *232*, 52–59. [CrossRef]

86. Zor, E.; Bekar, N. Lab-in-a-syringe using gold nanoparticles for rapid colorimetric chiral discrimination of enantiomers. *Biosens. Bioelectron.* **2017**, *91*, 211–216. [CrossRef]

87. Muñoz, J.; Campo, A.G.; Riba-Moliner, M.; Baeza, M.; Mas-Torrent, M. Chiral magnetic-nanobiofluids for rapid electrochemical screening of enantiomers at a magneto nanocomposite graphene-paste electrode. *Biosens. Bioelectron.* **2018**, *105*, 95–102. [CrossRef]

88. Jafari, M.; Tashkhourian, J.; Absalan, G. Chiral recognition of tryptophan enantiomers using chitosan-capped silver nanoparticles: Scanometry and spectrophotometry approaches. *Talanta* **2018**, *178*, 870–878. [CrossRef]

89. Zor, E. Silver nanoparticles-embedded nanopaper as a colorimetric chiral sensing platform. *Talanta* **2018**, *184*, 149–155. [CrossRef]

90. Wang, Y.; Rao, Z.; Zhou, J.; Zheng, L.; Fu, L. A chiral assembly of gold nanoparticle trimer-based biosensors for ultrasensitive detection of the major allergen tropomyosin in shellfish. *Biosens. Bioelectron.* **2019**, *132*, 84–89. [CrossRef]

91. Zhou, X.; Xu, C.; Jin, Y.; Li, B. Visual chiral recognition of D/L-leucine using cube-shaped gold nanoparticles as colorimetric probes. *Spectrochim. Acta Part A Mol. Biomol. Spectrosc.* **2019**, *223*, 117263. [CrossRef]

92. Zhang, Q.; Fu, M.; Lu, H.; Fan, X.; Wang, H.; Zhang, Y.; Wang, H. Novel potential and current type chiral amino acids biosensor based on L/D-handed double helix carbon nanotubes@polypyrrole@Au nanoparticles@L/D-cysteine. *Sens. Actuators B Chem.* **2019**, *296*, 126667. [CrossRef]

93. Sun, Y.; Zhao, H.; Boussouar, I.; Zhang, F.; Tian, D.; Li, H. Highly sensitive chiral sensing by calix[4]arene-modified silver nanoparticles via dynamic light scattering. *Sens. Actuators B Chem.* **2015**, *216*, 235–239. [CrossRef]

94. Song, G.; Xu, C.; Li, B. Visual chiral recognition of mandelic acid enantiomers with l-tartaric acid-capped gold nanoparticles as colorimetric probes. *Sens. Actuators B Chem.* **2015**, *215*, 504–509. [CrossRef]